Drift-Free Inertial Sensor-Based Joint Kinematics for Long-Term Arbitrary Movements

Ive Weygers, Manon Kok, Henri De Vroey, Tommy Verbeerst, Mark Versteyhe, Hans Hallez, and Kurt Claeys

***Abstract*—The ability to capture joint kinematics in outside-laboratory environments is clinically relevant. In order to estimate kinematics, inertial measurement units can be attached to body segments and their absolute orientations can be estimated. However, the heading part of such orientation estimates is known to drift over time, resulting in drifting joint kinematics. This study proposes a novel joint kinematic estimation method that tightly incorporates the connection between adjacent segments within a sensor fusion algorithm, to obtain drift-free joint kinematics. Drift in the joint kinematics is eliminated solely by utilizing common information in the accelerometer and gyroscope measurements of sensors placed on connecting segments. Both an optimization-based smoothing and a filtering approach were implemented. Validity was assessed on a robotic manipulator under varying measurement durations and movement excitations. Standard deviations of the estimated relative sensor orientations were below 0.89° in an optimization-based smoothing implementation for all robot trials. The filtering implementation yielded similar results after convergence. The method is proven to be applicable in biomechanics, with a prolonged gait trial of 7 minutes on 11 healthy subjects. Three-dimensional knee joint angles were estimated, with mean RMS errors of 2.14°, 1.85°, 3.66° in an optimization-based smoothing implementation and mean RMS errors of 3.08°, 2.42°, 4.47° in a filtering implementation, with respect to a golden standard optical motion capture reference system.**

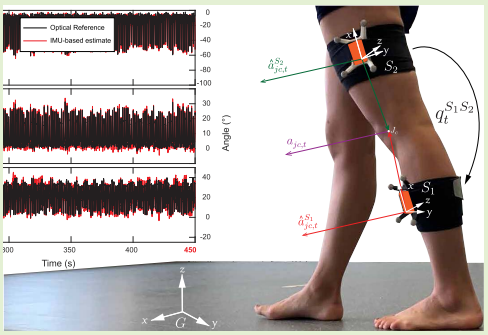

***Index Terms*—Body sensor networks, gait, inertial-sensor drift, motion analysis, sensor fusion, wearable sensors.**

I. Introduction

INTEREST in outside-laboratory movement analysis with inertial sensors (i.e. accelerometer and gyroscope) is increasing [1], [2]. Optoelectronic camera-based systems are currently known as the golden standard in biomechanical analysis [3]. Unlike artificial laboratory situations, inertial sensor-based methods can provide a way to measure kinematics in comfortable outdoor settings, omitting restrictions in physical space [4]. In this work we propose a novel tightly coupled sensor fusion algorithm for joint kinematic estimation (e.g. the knee joint as depicted in Fig. 1) from inertial measurements. We aim to make inertial sensors applicable to long-term human motion analysis in challenging outside laboratory environments, i.e. on a sports field or a hospital environment.

Inertial sensor-based methods typically require one sensor unit to be attached to adjacent segments around a joint of interest [2]. In order to estimate joint kinematics, the absolute three-dimensional (3-D) orientation of both inertial sensors is required. By fusing different sources of orientation information from sensor measurements, an accurate sensor orientation estimate can be obtained [5]. Angular velocity yields information on the change of orientation, after an integrating step. These relative sensor orientation estimates are accurate over short time periods but drift over time, due to the integration of noise and a non-zero gyroscope bias. Accelerometers are used as a measure of gravity to

Manuscript received January 10, 2020; revised March 18, 2020; accepted March 18, 2020. Date of publication March 23, 2020; date of current version June 18, 2020. This work was supported by the European Regional Development Fund under Project 1047': (We-Lab for Health, Technology and Movement). The associate editor coordinating the review of this article and approving it for publication was Prof. Kea-Tiong Tang. *(Corresponding author: Ive Weygers.)*

Ive Weygers, Henri De Vroey, and Kurt Claeys are with the Department of Movement and Rehabilitation Sciences, KU Leuven Campus Bruges, 8200 Bruges, Belgium (e-mail: ive.weygers@kuleuven.be; henri.devroey@kuleuven.be; kurt.claeys@kuleuven.be).

Manon Kok is with the Department of Mechanical, Maritime and Materials Engineering, TU Delft, 2628 Delft, The Netherlands (e-mail: m.kok-1@tudelft.nl).

Tommy Verbeerst is with the Department of Electrical Engineering, KU Leuven Campus Bruges, 8200 Bruges, Belgium (e-mail: tommy.verbeerst@kuleuven.be).

Mark Versteyhe is with the Department of Mechanical Engineering, KU Leuven Campus Bruges, 8200 Bruges, Belgium (e-mail: mark.versteyhe@kuleuven.be).

Hans Hallez is with the Department of Computer Sciences, KU Leuven Campus Bruges, 8200 Bruges, Belgium (e-mail: hans.hallez@kuleuven.be).

Digital Object Identifier 10.1109/JSEN.2020.2982459

Fig. 1. Experimental setup: Two inertial sensors are attached to thigh and shank body segments. Reference coordinate frames (blue) R_1 and R_2 are formed by clusters of optical markers that follow the movements of inertial sensor coordinate frames (white) S_1 and S_2. Sensor orientations are estimated with respect to a global coordinate reference frame G and reference orientations are obtained with respect to a Vicon base coordinate frame B.

compensate for drift in the tilt angle of the orientation estimates [6]. The heading angle of such estimates is still unknown and will drift over time. To compensate for this drift, an absolute measure of heading from 3-D magnetometers can be used [7], [8]. However, near ferro-magnetic material and electronic devices, the magnetic field vector is disturbed, which makes magnetometers unusable in many clinical settings such as a hospital environment [9]–[11]. Furthermore, the magnetic disturbance typically varies at different physical sensor locations in a non-homogenous magnetic environment.

Long-term stable sensor orientation estimates are impossible without absolute sensor heading information. However, previous studies have shown stable joint kinematic estimates, while omitting magnetometer measurements, by combining measurements of multiple inertial sensors and constraints for different joint kinematic models:

For joints that are modeled to have one Degree of Freedom (DoF), Dejnabadi *et al.* [12] proposed a method for the calculation of knee flexion and extension joint angles by describing acceleration measurements of adjacent segments at the joint center. Furthermore, Dorschky *et al.* [13] proposed a method to estimate planar gait and running kinematics as well as kinetics from inertial measurements. The obtained kinematics were insensitive to drift, due to translating inertial measurements from body segments to a virtual sensor at the joint center.

For joints with two DoF, Laidig *et al.* [14] recently proposed an inertial motion tracking method with an orientation-based constraint that overcomes the need for magnetometer measurements. Long-time stable and drift-free relative orientations and joint angles were tracked.

For joints that are modeled to have three degrees of freedom, Fasel *et al.* [15] combined information from multiple inertial sensors to obtain drift-free 3-D segment orientations and joint angles, suitable for highly dynamic movements. Joint-center positions were estimated and drift in connecting segments was estimated and removed from proximal to distal connecting sensor. Lee *et al.* [16] proposed a method to compensate for relative heading drift between sensors. After separately estimating the pitch and roll of two sensors [17], a second Kalman filter exploited information on the link between segments to improve the relative orientation between sensors. Roetenberg *et al.* [18] incorporated the position of the joint center in the sensor dynamics to correct for drift in the joint angle. Kok *et al.* [19] incorporated position and velocity in the dynamic model, combined with a biomechanical constraint to keep adjacent segments connected, at all times. This resulted in drift-free joint angles.

In previous studies, joint kinematics for 3 DoF joints is usually obtained in a decentralized manner. For example, by estimating a drift trend and adapting drift-affected orientation estimates afterwards [15] or by combining parts of the orientation estimates from multiple cascade Kalman filters [16], [17]. Such loosely coupled approaches consist of sequential steps that use little or no knowledge from previous steps. This could result in a loss of certainty and accuracy between steps [20]. Also, experimental validation has been carried out on rigid mechanical setups with joints that match ideal assumptions [16] or is restricted to segment inclination in a dominant sagittal movement plane [15]. Including position and velocity [19] makes the problem more computationally heavy and extensive validation is necessary for a good understanding of the working principles [18].

In the present study, we propose a novel joint kinematic estimation method that eliminates drift in the 3-D relative movement between two inertial sensors. Drift in the joint kinematics is eliminated solely by utilizing common information in the accelerometer and gyroscope measurements of sensors placed on connecting segments. The main contributions of this work include the following:

1) In contrast to loosely coupled approaches, we tightly couple rigid body kinematics within the sensor fusion algorithm to compensate for drift in the joint kinematics.

2) Extensive validation is carried out in three movement planes with respect to an industrial robotic manipulator. Moreover, a prolonged gait trial of 7 minutes, on 11 healthy subjects shows applicability in biomechanics and robustness against inter-subject gait variances, with respect to a golden standard optical motion capture reference system.

3) In addition to an optimization implementation, a filtering approach is presented that opens up for longer real-world studies.

The remaining contribution is organized as follows: In Section II, models are described that couple the orientation of two segments and thereby compensate for drift in the estimated relative sensor orientation. In Section III, an optimization-based smoothing and a filtering algorithm are presented that use the models from Section II to estimate the sensor orientations. In Section IV, experimental validation

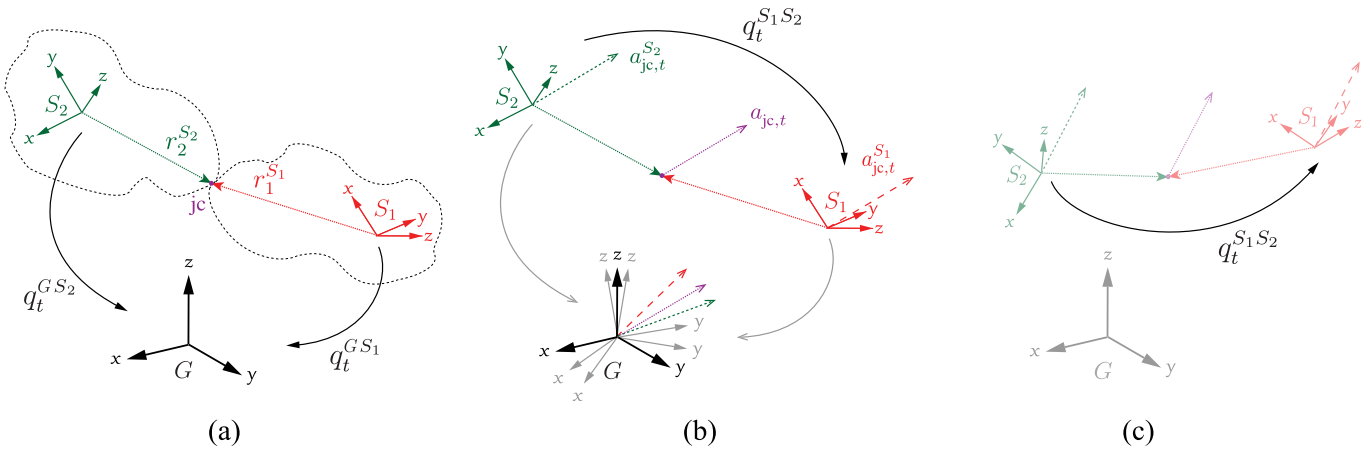

Fig. 2. Models and intuition: (a) Kinematic model with two inertial sensors S_1 and S_2, attached to segments that connect at the joint center jc by a spherical joint. (b) Joint center acceleration $a_{\text{jc},t}$ expressed in both sensor coordinate frames $a_{\text{jc},t}^{S_1}$, $a_{\text{jc},t}^{S_2}$ and their projection onto a common, but drifting global coordinate frame G. (c) The relative orientation between segments $q^{S_1S_2}$ is independent of a reference coordinate frame G.

on a robotic manipulator gives understanding to the proposed method. In Section V, applicability of the method in biomechanics is evaluated for a long-term gait trial on healthy subjects. Section VI discusses the obtained results.

II. Models

Joint kinematics is characterized as the study of the relative motion of two consecutive body segments of the human body [21]. Such a system can be modeled as two adjacent rigid segments, connected by a spherical joint with no restrictions in terms of rotational DoF.

In our model, each segment consists of an inertial sensor with coordinate frame S_i (Fig. 2 (a)) where a subscript index i (with $i = 1, 2$) differentiates between individual sensor coordinate frames. Two adjacent segments connect at a common point, the joint center jc. In the direction of this point, position vectors $r_i^{S_i}$ are defined from each sensor coordinate frame origin. Orientations are expressed in unit quaternion and direct cosine matrix notations. For example, $q_t^{GS_2}$ and $R_t^{GS_2}$ both describe the orientation of sensor coordinate frame S_2 with respect to the global coordinate frame G at time index t.

A. Dynamic Model

Inertial sensors are commonly used for orientation estimation from gyroscope and accelerometer measurements [5]. The sensor's angular velocity $\omega_t^{S_i}$ is measured by the gyroscope $y_{\omega,t}^{S_i}$ and modeled at each time instant t with $t = 1, \ldots, N$ as

$$y_{\omega,t}^{S_i} = \omega_t^{S_i} + e_{\omega,t}^{S_i}, \tag{1}$$

where $e_{\omega,t}^{S_i}$ is zero-mean Gaussian noise, distributed as $\mathcal{N}(0, \Sigma_\omega)$. We define the gyroscope noise covariance as $\Sigma_\omega = \sigma_\omega^2 \mathcal{I}_3$, where $\mathcal{I}_3$ describes the 3×3 identity matrix and N is the total number of samples in the process. Scale factors and non-orthogonality in the sensor axes are assumed to be negligible due to calibration by the manufacturer. The individual absolute sensor orientations $q_t^{GS_i}$, can be estimated following dynamic model

$$q_t^{GS_i} = q_{t-1}^{GS_i} \odot \frac{T}{2} \overline{y}_{\omega,t}^{S_i}, \tag{2}$$

where the measured angular velocity $y_{\omega,t}^{S_i}$ is integrated over a time step T, to estimate the change in orientation from $q_{t-1}^{GS_i}$ to $q_t^{GS_i}$. The $\odot$ operator in (2) denotes a quaternion multiplication and $\overline{y}_{\omega,t}^{S_i}$ describes a pure quaternion notation of the vector $y_{\omega,t}^{S_i}$ [22].

B. Measurement Model

Orientation estimates from gyroscope measurements are known to be accurate for short time periods, but drift over time [5]. To remove this drift, orientation estimates can be updated by using measurements of acceleration $y_{a,t}^{S_i}$ that are modeled as

$$y_{a,t}^{S_i} = R_t^{S_iG}(a^G - g^G) + e_{a,t}^{S_i}, \tag{3}$$

where g^G denotes the gravity component, a^G denotes the linear acceleration component and $R^{S_iG} = (R^{GS_i})^{\mathrm{T}}$.

We make use of common information present in the gyroscope and accelerometer measurements of two adjacent inertial sensors to update both orientations $R_t^{GS_1}$ and $R_t^{GS_2}$ together, in order to compensate for drift in the joint angle $R_t^{S_1S_2}$. From rigid body kinematics we learn that the acceleration of a common point i.e. the joint center, should have only one unique description of acceleration $a_{\text{jc},t}^{S_i}$ in a common reference coordinate frame (Fig. 2 (b)), which can be expressed as

$$R_t^{GS_1} a_{\text{jc},t}^{S_1} = R_t^{GS_2} a_{\text{jc},t}^{S_2} + e_{\text{link},t}, \tag{4}$$

where $e_{\text{link},t} \sim \mathcal{N}(0, \Sigma_{\text{link}})$. Joint center accelerations $a_{\text{jc},t}^{S_1}$ and $a_{\text{jc},t}^{S_2}$ are approximated by evaluating acceleration measurements $y_{a,t}^{S_i}$ at a distance $r_i^{S_i}$ from the joint center by using $\mathcal{C}_t^{S_i}$ as

$$\begin{aligned} a_{\text{jc},t}^{S_i} &= y_{a,t}^{S_i} - \mathcal{C}_t^{S_i} r_i^{S_i}, \\ \mathcal{C}_t^{S_i} &= [y_{\omega,t}^{S_i}\times]^2 + [\dot{y}_{\omega,t}^{S_i}\times]. \end{aligned} \tag{5}$$

Here, the operator $\times$ describes a cross product matrix formulation and $\dot{y}_{\omega,t}^{S_i}$ denotes angular accelerations. Joint center position vectors $r_i^{S_i}$ are estimated from inertial

Filt.-algorithm 1: Joint Kinematic Estimation

Input: Inertial sensor data $\{y_{a,t}^{S_i}, y_{\omega,t}^{S_i}\}_{t=1}^{N}$ for $i = 1, 2$, an initial orientation estimate $\tilde{q}_{1|1}^{GS_i}$ for $i = 1, 2$, covariance matrices $P_{1|1}$, Q, and R.
Output: Orientation estimate $\hat{q}_{1:N}^{GS_i}$, for $i = 1, 2$.

1: Approximate $r_1^{S_1}$, $r_2^{S_2}$ as in [23].
2: **for** t = 2, …, N **do**
3: Approximate $a_{\text{jc},t}^{S_1}$, $a_{\text{jc},t}^{S_2}$ following model (5).
4: **Time update**
5: $\tilde{q}_{t|t-1}^{GS_i} = \tilde{q}_{t-1|t-1}^{GS_i} \odot \exp_q(T2^{-1} y_{w,t-1}^{S_i})$, for $i = 1, 2$.
6: $P_{t|t-1} = F_{t-1} P_{t-1|t-1} F_{t-1}^{\mathrm{T}} + GQG^{\mathrm{T}}$
7: **Measurement update**
8: $S_t = H_t P_{t|t-1} H_t^{\mathrm{T}} + R$
9: $K_t = P_{t|t-1} H_t^{\mathrm{T}} S_t^{-1}$
10: $\hat{\eta}_t = K_t e_{\text{link},t}$
11: **Relinearize**
12: $\tilde{q}_t^{GS_i} = \tilde{q}_t^{GS_i} \odot \exp_q(\hat{\eta}_{S_i,t} 2^{-1})$, for $i = 1, 2$.
13: $P_{t|t} = J_t(P_{t|t-1} - K_t S_t K_t^{\mathrm{T}}) J_t^{\mathrm{T}}$
14: $\hat{q}_t^{GS_i} = \tilde{q}_t^{GS_i}$, for $i = 1, 2$.
15: **end for**

Opt.-algorithm 2: Joint Kinematic Estimation

Input: Inertial sensor data $\{y_{a,t}^{S_i}, y_{\omega,t}^{S_i}\}_{t=1}^{N}$ for $i = 1, 2$, an initial orientation estimate $\tilde{q}^{GS_i,(0)})_{1:N}$ for $i = 1, 2$, covariance matrices Σ_{init}, Σ_{ω}, and Σ_{link}.
Output: Orientation estimate $\hat{q}_{1:N}^{GS_i}$, for $i = 1, 2$.

1: Approximate $r_1^{S_1}$, $r_2^{S_2}$ as in [23] and $a_{\text{jc},1:N}^{S_1}$, $a_{\text{jc},1:N}^{S_2}$ following model (5).
2: Set k = 0.
3: **while** *termination condition is not satisfied* **do**
4: Compute: $\varepsilon = \left[(\varepsilon_{\text{init}}^{S_1})^{\mathrm{T}} \; (\varepsilon_{\omega}^{S_1})^{\mathrm{T}} \; (\varepsilon_{\text{init}}^{S_2})^{\mathrm{T}} \; (\varepsilon_{\omega}^{S_2})^{\mathrm{T}} \; (\varepsilon_{\text{link}})^{\mathrm{T}}\right]^{\mathrm{T}}$.
5: Compute: $\mathcal{J}$, $\mathcal{G} = \mathcal{J}^{\mathrm{T}}\varepsilon$, $\hat{\mathcal{H}} \approx \mathcal{J}^{\mathrm{T}}\mathcal{J}$.
6: set $\hat{\eta}_{1:N}^{(k+1)} = -\hat{\mathcal{H}}^{-1}\mathcal{G}$.
7: **Relinearize**
8: $\tilde{q}_t^{GS_i,(k+1)} = \tilde{q}_t^{GS_i,(k)} \odot \exp_q(\hat{\eta}_{S_i,t}^{(k+1)} 2^{-1})$, for $i = 1, 2$.
9: $k \leftarrow k + 1$.
10: **end while**
11: Set $\hat{q}_{1:N}^{GS_i} = \tilde{q}_{1:N}^{GS_i,k}$, for $i = 1, 2$.

measurement data as proposed by Seel *et al.* [23], under the assumption that segments are rigid.

Conventional methods [5], [6] assume a dominant gravity component and approximating zero linear acceleration component to compensate for drift in the tilt part of the orientation estimates. In contrast, the proposed measurement model (4) yields orientation information in three movement planes rather than only in the tilt part, as long as there is acceleration. We will explicitly use this information in Section III to obtain drift-free 3-D joint kinematics.

III. Estimation of Joint Kinematics

Models from Section II are implemented in a filtering (Filt.-algorithm 1) and an optimization-based smoothing approach (Opt.-algorithm 2). The smoothing algorithm uses all measurements $\{y_{a,t}^{S_i}, y_{\omega,t}^{S_i}\}_{t=1}^{N}$ in each iteration, to obtain the most accurate estimates. The filtering algorithm on the other hand opens up for on-line implementations.

We adopt the orientation parameterization from [5] to encode orientations $q_t^{GS_i}$ in terms of an orientation deviation state vector $\eta_t \in \mathbb{R}^3$ around a linearization point $\tilde{q}_t^{GS_i}$. For our two-sensor kinematic model we define the state as $\eta_t = \left[\eta_{\text{S}_1,t}^{\mathrm{T}} \; \eta_{\text{S}_2,t}^{\mathrm{T}}\right]^{\mathrm{T}} \in \mathbb{R}^6$. Joint center position vectors $r_i^{S_i}$ are estimated from inertial measurement data as proposed by Seel *et al.* [23], under the assumption that segments are rigid. Moreover, angular accelerations $\dot{y}_{\omega,t}^{S_i}$ are approximated from gyroscope measurements by means of a five-point finite difference approximation.

A. Filtering

Our filtering algorithm to estimate joint kinematics is summarized in Filt.-algorithm 1. It extends the multiplicative extended Kalman filter from [5] to estimate the orientation of two sensors and to incorporate the model (4).

Sensor dynamics recursively propagate measurements of the angular velocity $y_{w,t}^{S_i}$ through the states (step 5) and the state covariances P_t (step 6). Orientation estimates of both sensors are simultaneously updated using measurement model (4) (steps 8-10). To derive H_t, the Jacobian of the measurement model (4) with respect to the state, we first note that $R_t \approx \tilde{R}_t(\mathcal{I}_3 + [\eta\times])$ by assuming η_t to be small [5]. Measurement model (4) can therefore be written in terms of the state η_t as

$$\begin{aligned} &\tilde{R}_t^{GS_1}(\mathcal{I}_3 + [\eta_{S_1,t}\times]) a_{\text{jc},t}^{S_1} \\ &\quad \approx \tilde{R}_t^{GS_2}(\mathcal{I}_3 + [\eta_{S_2,t}\times]) a_{\text{jc},t}^{S_2} + e_{\text{link},t}. \end{aligned} \tag{6}$$

Hence the matrix $H_t \in \mathbb{R}^{3\times 6}$ is given by

$$H_t = \left(\tilde{R}_t^{GS_1}[a_{\text{jc},t}^{S_1}\times] - \tilde{R}_t^{GS_2}[a_{\text{jc},t}^{S_2}\times]\right). \tag{7}$$

Additionally, the linearization point is updated as well as the covariance around this updated linearization point (steps 12-13). Note that the $\exp_q$ operator denotes the vector exponential map i.e. $v \in \mathbb{R}^3 \rightarrow q \in \mathbb{R}^4$ [6] and steps 5, 12, and 14 apply to both sensors.

B. Optimization

Instead of using measurements up to the current time-step (Filt.-algorithm 1) and iteratively calculating the state, in Opt.-algorithm 2, we also present an optimization-based smoothing approach. Since the noise in (2) and (4) is Gaussian, this reduces to a weighted least-squares problem which we solve using a Gauss-Newton approach [24]. Each Gauss-Newton iteration k, makes use of all measurements

TABLE I
MEAN $\overline{\sigma}$ AND MAX σ FROM THE ESTIMATED AVERAGE JOINT CYCLE OVER ALL CYCLES FOR ALL ROBOT TRIALS

Trial	Duration	Speed	Filt.-algorithm						Opt.-algorithm					
			ϕ (°)		ψ (°)		θ (°)		ϕ (°)		ψ (°)		θ (°)	
	(s)	(mm/s)	$\overline{\sigma}$	max σ	$\overline{\sigma}$	max σ	$\overline{\sigma}$	max σ	$\overline{\sigma}$	max σ	$\overline{\sigma}$	max σ	$\overline{\sigma}$	max σ
1	10	1500	0.82	1.60	0.77	1.25	1.18	2.78	0.80	1.97	0.57	1.11	0.54	1.57
2	60	1500	0.72	1.45	0.58	1.07	0.67	1.52	0.66	1.56	0.47	0.90	0.43	1.39
3	300	1500	0.68	1.52	0.50	0.98	0.49	1.44	0.69	1.63	0.48	0.94	0.44	0.14
4	10	200	5.07	9.03	5.28	10.55	9.76	16.25	0.45	0.86	0.38	0.86	0.60	1.25
5	60	200	2.78	4.93	2.85	5.53	4.98	8.06	0.40	0.80	0.30	0.74	0.35	0.73
6	300	200	2.61	4.27	3.10	5.97	6.25	10.06	0.42	0.76	0.37	0.82	0.51	0.90
7	10	50	0.77	4.09	0.74	1.89	1.03	4.42	0.18	0.45	0.22	0.42	0.64	1.06
8	60	50	3.58	7.68	3.92	7.71	7.77	14.49	0.33	0.62	0.45	0.69	0.88	1.33
9	300	50	1.98	4.11	2.14	4.18	4.16	8.01	0.49	1.14	0.61	1.00	0.74	1.45

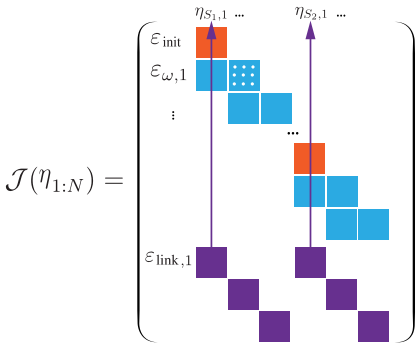

Fig. 3. Illustration of the Jacobian structure for joint kinematic estimation. The white dots denote the 3×3 size of each part in the Jacobian matrix. Due to the tightly coupled nature of the algorithm, the measurement model (purple) is allowed to directly adapt the orientation estimates of both sensors at all time, to keep segments connected. Sensor dynamics (blue) yield information on current and previous orientation estimates. A prior initial orientation estimate (orange) can be adapted during different Gauss-Newton iterations.

$\{y_{a,t}^{S_i}, y_{\omega,t}^{S_i}\}_{t=1}^{N}$ to calculate the objective function as

$$\hat{\eta}_{1:N} = \underset{\hat{\eta}_{1:N}}{\arg\min} \sum_{i=1}^{2} \Bigg(\underbrace{\|e_{\text{init}}^{S_i}\|^2_{\Sigma_{\text{init}}^{-1}}}_{\text{Initial}} + \underbrace{\sum_{t=2}^{N} \|e_{\omega,t}^{S_i}\|^2_{\Sigma_{\omega}^{-1}}}_{\text{Dynamics}} \Bigg) + \underbrace{\sum_{t=1}^{N} \|e_{\text{link},t}\|^2_{\Sigma_{\text{link}}^{-1}}}_{\text{Measurement model}}, \tag{8}$$

where $\|e\|^2_{\Sigma^{-1}}$ weighs the cost e according to its noise covariance as $\varepsilon = \Sigma^{-1/2} e$. We refer to [5] for the objective functions regarding the initial orientation estimates $e_{\text{init}}^{S_i}$ and the sensor dynamics $e_{\omega,t}^{S_i}$, with their corresponding derivatives and covariance matrices Σ_{init}, Σ_{ω}. The objective function is then evaluated on the current linearization point $\tilde{q}_{1:N}^{GS_i,(k)}$ (step 4). Objective functions are appraised with respect to the state by calculating the Jacobian $\mathcal{J}$ in (step 5) (Fig. 3) with the following derivatives for the link between segments

$$\begin{aligned} \frac{de_{\text{link},t}}{d\eta_{S_1,t}} &\approx -\tilde{R}_t^{GS_1}[a_{\text{jc},t}^{S_1}\times], \\ \frac{de_{\text{link},t}}{d\eta_{S_2,t}} &\approx \tilde{R}_t^{GS_2}[a_{\text{jc},t}^{S_2}\times]. \end{aligned} \tag{9}$$

Search direction and step size are defined by the gradient $\mathcal{G}$ and approximated Hessian $\hat{\mathcal{H}}$, to update the state (step 6). The linearization points are updated (step 8) before each new iteration. Note that steps 8 and 11 apply to both sensors.

IV. EXPERIMENTAL VALIDATION

A. Measurement Setup

Experimental validation was done on a 6-DoF industrial robotic manipulator (ABB IRB 120) where two inertial sensors (MTw Awinda, Xsens) were attached on the robot via Velcro strips (Fig. 5). To mimic arbitrary movements, the end effector was imposed to draw an eight-shaped trajectory with varying maximum end effector speeds and time durations, as described in Table I. An industrial robotic manipulator is capable of performing the exact same movement pattern, multiple times. It is therefore possible to assess both drift and accuracy of the orientation estimates by comparing different cycles of a trial.

All trials were processed using Filt.-algorithm 1 and Opt.-algorithm 2, that were implemented in a custom Matlab (R2018a, Mathworks, USA) script. A static time period of 5 seconds at the beginning of each experiment is used to correct for a gyroscope bias and to empirically define noise variance σ_{ω}^2 to fill matrices Σ_{ω} and Q. Initial orientations $\tilde{q}_{1|1}^{GS_i}$, $\tilde{q}^{GS_i,(0)})_{1:N}$ were set to $[1\ 0\ 0\ 0]^{\text{T}}$ and initial process covariance $P_{1|1}$ was set to $\mathcal{I}_6$. Measurement noise covariance matrix R and covariance matrix Σ_{link} were chosen to be $\mathcal{I}_3$.

B. Accuracy in Varying Excitation and Measurement Duration

After processing all trials, joint angle estimates are obtained following

$$\hat{q}_t^{S_1S_2} = (\hat{q}_t^{GS_1})^c \odot \hat{q}_t^{GS_2}, \tag{10}$$

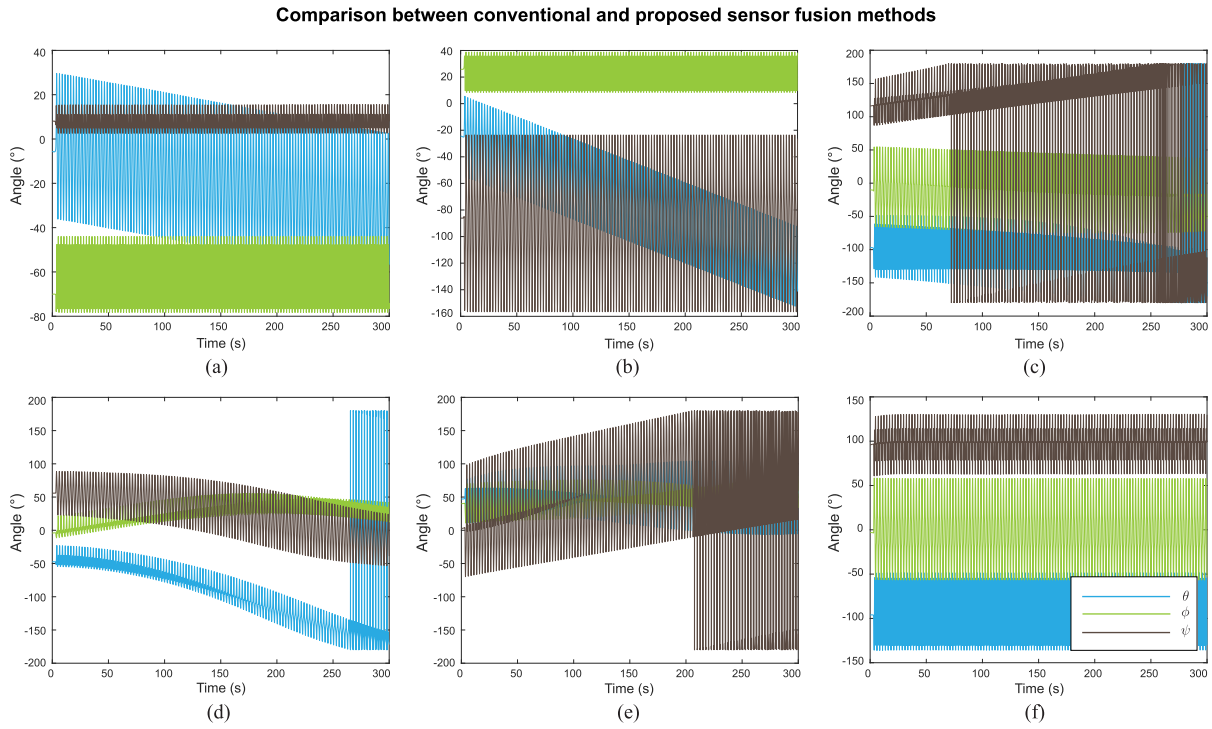

Fig. 4. A comparison between the conventional and the proposed sensor fusion scheme for robot trial 6: Resulting absolute orientation estimates $q_t^{GS_1}$ (a, d), $q_t^{GS_2}$ (b, e), and relative orientations $q_t^{S_2S_1}$ (c, f) (Euler representation). In conventional methods for orientation estimation (a-c), absolute orientation estimates (a-b) drift in the heading part when only gyroscope and accelerometer data are used. When making use of rigid body kinematics and approximating joint center accelerations in the measurement update of the proposed method (d-f), absolute sensor orientations (d, e) will drift in pitch, roll, and yaw, but relative orientations (f) become consistent.

were the c operator denotes the quaternion conjugate. In order to discuss all resulting joint angle estimates for the longest robot trials 3 (with the fastest movement excitation) and 9 (with the slowest movement excitation), a peak-finding algorithm divides each trial of size $3 \times N$ (Euler representation) in C cycles, each of size $3 \times (N/\mathrm{C})$. A sample by sample average cycle $\overline{\mathrm{C}}$ is obtained from all cycles. The deviation of all cycles in C from $\overline{\mathrm{C}}$ at each time instance can be expressed as standard deviations (σ) (Fig. 6). Mean ($\overline{\sigma}$ and maximum (max σ) standard deviations are reported in Table I.

Fig. 4 shows a comparison between the conventional and the proposed sensor fusion scheme for robot trial 6. It illustrates how the proposed model adapts both absolute sensor orientations in such a way that relative orientation estimates improve. The optimization-based smoothing yields the best results compared to a filtering implementation, with standard deviations under 0.89° and maximum standard deviations up to 1.97°. We can conclude that even in absence of absolute heading information, accelerometer readings are sufficient to keep both segments drifting together (as illustrated in Fig. 2 (b, c)).

Even after 300 seconds of measurement, the estimated joint angles still coincide with standard deviations under 0.70°. We can conclude that measurement duration does not affect the algorithm outcome. Note that when movement excitation decreases (Trials 4-9), a filtering implementation yields greater deviations as shown in (Fig. 6, (b)). However, this deviation is not due to drifting estimates over time. An optimization-based smoothing implementation can adapt the initial orientation estimate by making use of all measurements, in multiple filter iterations. The filtering implementation only relies on accelerations and model (4) to be able to update the sensor orientation as shown in Fig. 7.

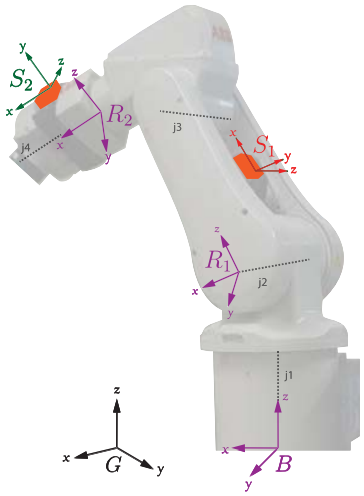

Fig. 5. Experimental validation: A 6-DoF industrial robotic manipulator (ABB IRB 120) moves in a predefined eight-shaped trajectory by actuating joint axes $j1 - j4$. Two inertial sensors S_1 and S_2 simultaneously capture the movement of robotic segments R_1 and R_2. Sensor orientations are estimated with respect to a global coordinate reference frame G and robot reference orientations are obtained with respect to a robot base coordinate frame B.

V. Application to Gait Analysis

We demonstrated that the proposed method is able to estimate consistent and drift-free 3-D joint kinematics, over long periods of time, with respect to an industrial robotic

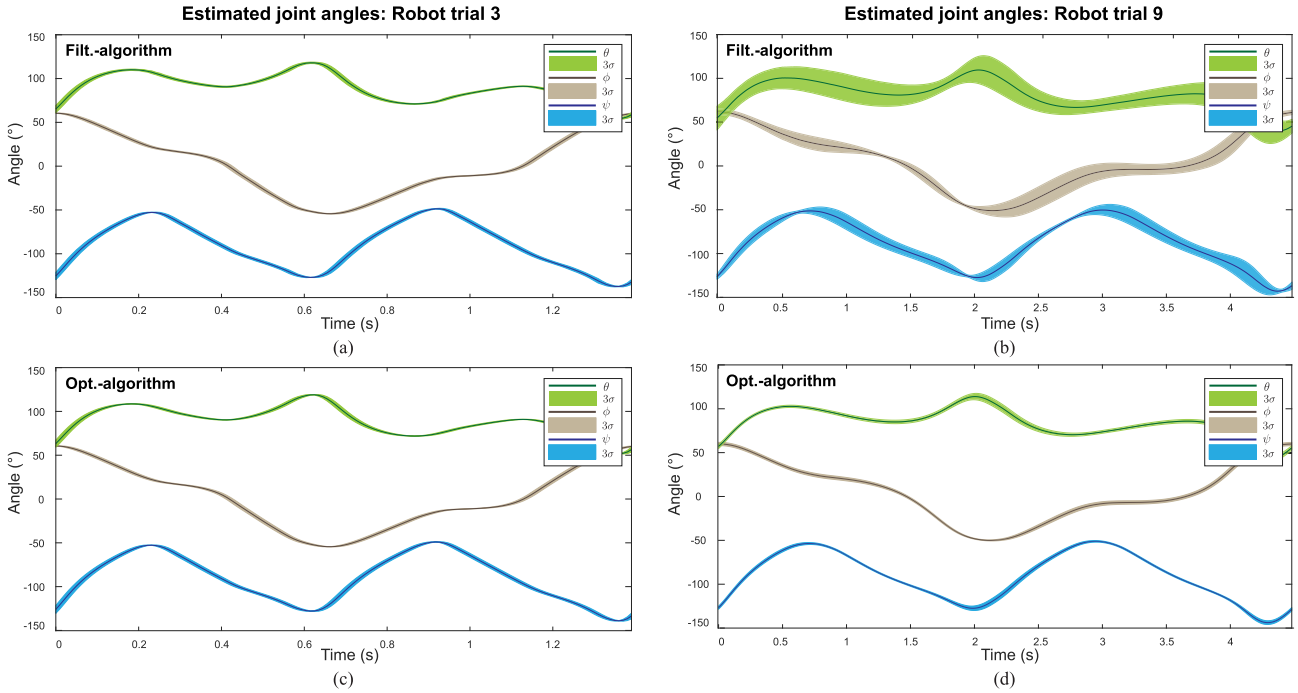

Fig. 6. Estimated joint angles (Euler representation) for robot trial 3, with the fastest movement excitation (a, c) and robot trial 9, with the slowest movement excitation (b, d). Solid lines summarizes all robot cycles in the trial as one mean cycle. The colored region around the solid lines describes the deviation of the estimates over time with 3σ bounds. Both Filt.-algorithm 1 (a, b) and Opt.-algorithm 2 (c, d) of the proposed method result in consistent estimates. High dynamic movements (a) result in high accelerations to preserve a fast convergence, even in a filtering implementation. Slow dynamic movements (b) need time to converge to consistent movement cycles in a filtering implementation, as illustrated in Fig. 7.

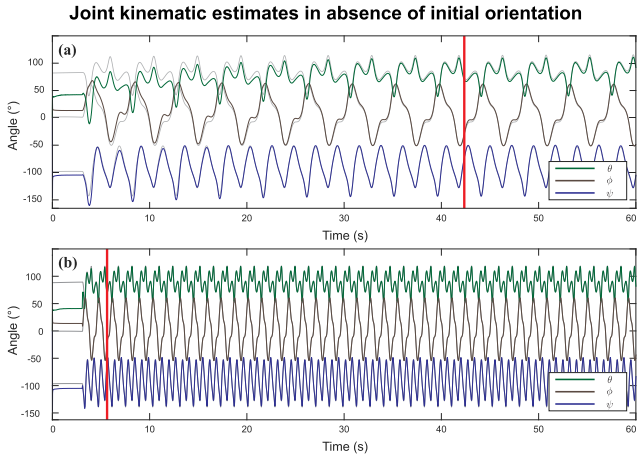

Fig. 7. Estimated joint angles for robot trial 8 (a) and robot trial 2 (b), in color (Opt.-algorithm 2) and gray (Filt.-algorithm 1). Over time both algorithms converge to the same estimate. The red line indicates when estimates from filtering and optimization-based smoothing coincide. In a filtering implementation, the time needed for this convergence depends on the dynamics of the motion. High dynamic movements (b) converge faster than slower movement dynamics (a).

manipulator. To evaluate the applicability in biomechanics, our method was applied to gait analysis.

A. Study Design

We evaluate our IMU-based joint kinematic estimation method against a gold-standard 3-D optical motion capture reference system. The inertial measurement-based method consisted of 2 inertial sensors (MTw Awinda, Xsens). The optical motion analysis reference system consisted of 13 infrared cameras (VICON Vero,Vicon Motion Systems Ltd). Both systems measured at a sample rate of 100Hz. Hardware time synchronization was used to simultaneously capture inertial measurements and marker trajectories. Joint kinematic estimates are computed in both an optimization-based smoothing manner and filtering approach, after capturing all data points. Measurement and process noise covariances were determined as described in Section IV-A.

Eleven healthy subjects (4 male and 7 female, age ranged between 18 and 57 years old, body mass index (BMI) ranged between 18.31 and 28.89) with no history of knee surgery prior to testing, gave their written informed consent. Inertial sensors were attached latero-cranial on the shank and on the lateral side at mid-distance on the thigh via Velcro strips. Custom 3-D-printed plastic cases with reflective marker clusters house the inertial sensors and therefore simultaneously capture the sensor orientation as a golden standard reference (as shown in Fig. 1).

At the beginning of the data acquisition, subjects were asked to stand still for 5 seconds. Afterwards, all subjects were told to walk arbitrarily in a comfortable self-selected pace for 7 minutes. During measurement, subjects could change their walking direction and speed.

The study has been approved by the institutional research committee of KU Leuven (Clinical trial center UZ Leuven, Nr. S58936). All tests were done in accordance with the 1964 Helsinki declaration and its later amendments.

B. Coordinate Frame Alignment

Sensor coordinate frames S_i and marker-based coordinate frames R_i will not be perfectly aligned due to unknown manual and sensor-to-case misalignments. Moreover, both

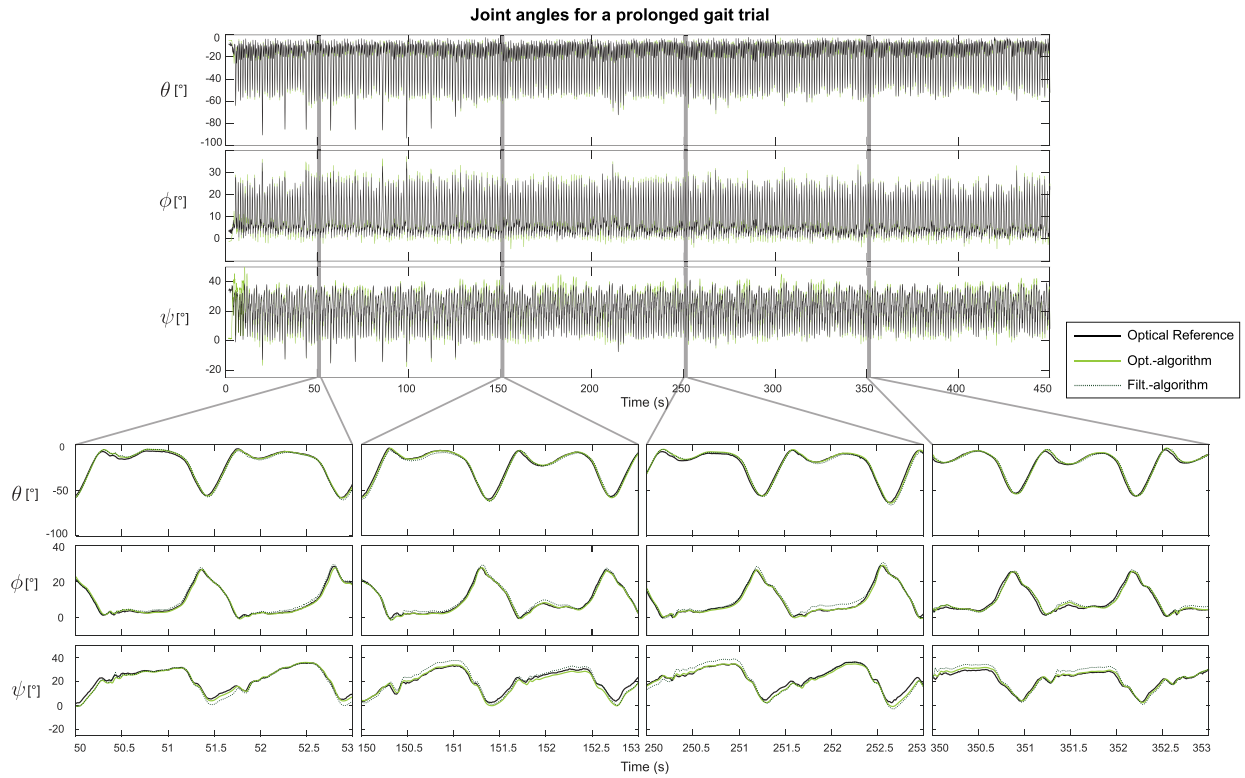

Fig. 8. Resulting 3-D knee joint angles for one subject, obtained from inertial sensor readings with the proposed method for joint kinematic estimation (green: Opt.-algorithm 2, dotted-green: Filt.-algorithm 1) and the optical reference (black) for a prolonged gait trial of 450 seconds. Results are plotted after coordinate frame alignment. Drift is clearly eliminated for the entire duration of the gait trial.

systems have different reference coordinate frames which do not align: sensor orientations are estimated with respect to a global coordinate reference frame G and clustered marker orientations are obtained with respect to a Vicon reference coordinate frame B as illustrated in Fig. 1.

To compare sensor orientation estimates ($\hat{q}_t^{GS_1}$, $\hat{q}_t^{GS_2}$) and Vicon reference orientations ($q_t^{BR_1}$, $q_t^{BR_2}$), constant misalignments $q^{R_2S_2}$ and $q^{R_1S_1}$ are estimated from relative orientation references $q_t^{R_1R_2}$ and relative orientation estimates $\hat{q}_t^{S_1S_2}$, by using the Theorem 4.2 from J.D. Hol [6]. Intuitively, the misalignment q^{GB} becomes irrelevant (as depicted in Fig. 2 (c)) when interest lies in the relative orientation, which can be formulated as

$$q^{S_1R_1} \odot q_t^{R_1R_2} \odot q^{R_2S_2} \approx q_t^{S_1G} \odot q^{GB} \odot q^{BG} \odot q_t^{GS_2},$$
$$q_t^{R_1R_2} \odot q^{R_2S_2} \approx q^{R_1S_1} \odot q_t^{S_1S_2}. \quad (11)$$

C. Data Analysis

In total, 11 optimizations and 11 filtering problems were solved. Processing a trial of 7 minutes (two inertial sensors measuring with a sample rate of 100Hz) by using Opt.-algorithm 2, typically converges after a couple iterations and takes about 15 minutes for an inefficient proof-of-concept Matlab implementation on 2 Xeon Gold 6140 CPUs@2.3 GHz (Skylake), 18 cores each. In comparison, Filt.-algorithm 1 takes about 9 seconds for a 7-minute trial. However, the matrix that needs inversion in the Gauss-Newton algorithm (Opt.-algorithm 2, step 6) is inherently sparse and can be solved efficiently in about 247ms.

We computed the coefficient of determination (R^2) between the estimated and reference relative sensor orientations (after coordinate frame alignment) using all time points from all subjects. In addition we used all data points and computed the ordinary least product regression and root-mean-squared errors (RMSE).

D. Results

Correlation between the optical reference and joint kinematic estimates, in both Filt.-algorithm 1 and Opt.-algorithm 2, for all subjects are illustrated in Fig. 9. Mean RMSE for all subjects were 2.14°, 1.85°, 3.66° in the optimization-based smoothing implementation and 3.08°, 2.42°, 4.47° in the filtering implementation. Maximum RMSE were 2.66°, 3.42°, 4.55° in the optimization-based smoothing implementation and 4.12°, 4.71°, 5.38° in the filtering implementation. Overall, correlations are above 0.9. The remaining variances are likely due to subject specific violations of the model assumptions on rigidity of body segments and small translational joint movements.

Fig. 8 shows the results for one subject with RMSE of 1.60°, 1.37°, 2.03° for an optimization implementation and RMSE of 2.18°, 1.58°, 3.12° for the filtering implementation, over the whole capture period. In addition, we zoom in on four time frames and report their RMSE in Table II. Drift is clearly eliminated for the entire duration of the gait trial.

VI. Discussion

The proposed method tightly couples rigid body kinematics within the sensor fusion algorithm, thereby eliminating drift

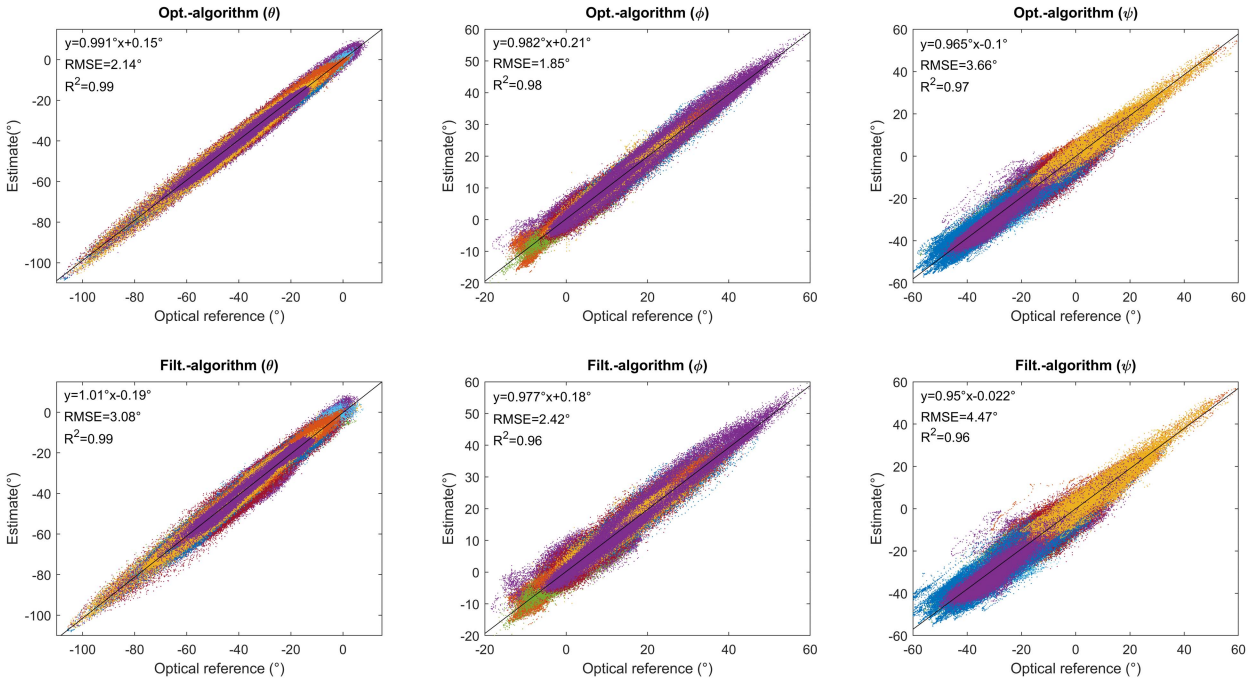

Fig. 9. Relative sensor orientation estimates (for both Filt.-algorithm 1 and Opt.-algorithm 2) and optical reference for eleven subjects walking for seven minutes. Correlation between orientation estimates and optical reference using ordinary least products regression, root-mean-square error (RMSE) and coefficient of determination R^2 are presented. Each correlation plot has 462000 points, from 11 subjects, each associated with a different color.

TABLE II
RMSE OF KNEE JOINT ANGLE ESTIMATES W.R.T. OPTICAL REFERENCE FOR ONE SUBJECT

Time Frame (s)	Method	θ (°)	ϕ (°)	ψ (°)
$[50-53]$	Opt.-algorithm	1.51	1.20	1.23
	Filt.-algorithm	2.11	1.55	1.94
$[150-153]$	Opt.-algorithm	1.59	1.37	1.99
	Filt.-algorithm	2.19	1.49	2.46
$[250-253]$	Opt.-algorithm	1.78	1.38	1.70
	Filt.-algorithm	2.08	1.83	2.88
$[350-353]$	Opt.-algorithm	1.60	1.39	1.29
	Filt.-algorithm	2.02	1.98	2.86

in the joint kinematic estimates. An intuitive explanation of the working principles is summarized in Fig. 2. Standard loosely coupled approaches [16] report RMSE of 3.04° over three minutes of measurement, on a two-link mechanical setup that matches idealistic model assumptions. Others report segment inclination errors of 3.9° for high dynamic movements over 90 seconds of measurements [15]. The tightly coupled nature of our proposed method achieves errors that are on average less than these reported in other studies, while being applied to arbitrary unconstrained human movements, over longer measurement durations. By estimating only the orientations of the sensors, rather than also their position and velocity [19], the problem becomes less computationally heavy to solve. This work more extensively validates the approach than existing state-of-the art [15], [16] on an accurate industrial robotic manipulator in Section IV. In addition, the application to gait analysis in Section V proves that our method is sufficient to eliminate drift, even in less-perfect conditions with possible soft-tissue artifacts and joint-translational movements, under varying movement speeds. Although the optimization-based implementation yields more accurate results, the filtering approach opens up for longer in-the-wild studies i.e. long term patient monitoring and smart garments.

The analysis of gait and functional movements outside of a laboratory can provide interesting clinical insides. The proposed method is currently applied to clinical gait analysis. During such movements, quasi-static time intervals occur where the inertial sensors are approximately a measure of gravity. In this state, the accelerometer measurements combined with the presented measurement model (4) do not yield information on the relative heading between sensors. Although the proposed method relies on the presence of acceleration, low dynamic activities such as gait proved to contain sufficient acceleration to correct for drift in the joint angle in Section V. A limitation of the current study might be the occurrence of shocks and vibrations which causes some special caution in sports applications [25]. The position of the sensor with respect to the joint center is assumed to be fixed, which does not allow for soft tissue artifacts. During these events joint position vectors become time-dependent, which has to be taken into account. However, during clinical gait analysis, this seems to be less of an issue. Note that the estimated joint angles do not reflect clinically relevant knee joint kinematics. Standardized reporting of joint motion asks for the identification of anatomical joint-axes following Grood and Suntay [26] and the International Society of Biomechanics (ISB) [27], [28].

However, methods that aim to identify these joint axes and overcome sensor-to-segment misalignments, often depend on accurate relative orientation estimates [29], [30].

We applied the presented method to clinical gait-analysis. However, further validation must be done to generalize to different functional movements such as lunges, walking stairs, or more highly dynamic movements with high angular velocities or persistent centripetal accelerations such as cycling or running. Moreover, the magnitude, direction, and frequency of occurrence of accelerations that are required to keep the heading stable will be topic of future work. The proposed sensor fusion scheme for connected segments can easily be scaled to multiple connecting segments. Fasel *et al.* [15] previously reported that direction errors in the joint position around 10° affected segment inclination and joint angle accuracy by less than 0.6°. Future research needs to be conducted to analyze the effects of errors in the estimated joint center position vectors on the kinematic estimates. Furthermore, future research might focus on uniquely jointly determining the relative sensor orientations and position vectors under certain types of motion. More efficient implementations can be achieved by exploiting the structure of the problem with tailored message passing [31] and by preintegration of inertial measurements [32] which is another direction of future work.

VII. Conclusion

A novel method that allows for the estimation of 3-D joint kinematics from inertial measurements was presented. The method requires one inertial sensor unit per adjacent segment around a joint of interest. Drift in the relative sensor orientation is compensated solely by exploiting common information in the accelerometer and the gyroscope measurements of the two sensors and rigid body kinematic equations.

Consistency in the kinematic estimates was evaluated with respect to an industrial robotic manipulator with excellent results under varying movement excitations and measurement durations. Although, the proposed method relies on the presence of acceleration, low dynamic activities such as gait was shown to contain sufficient acceleration to correct for drift in the joint angle. Further studies should include analysis of observability to clarify which motions are sufficient for the model to become manifest. Moreover, it needs to be investigated whether the estimation of model parameters e.g. joint position vectors [23] can be incorporated in the model.

The proposed algorithm allows us to perform long ($>$5 min) gait trials irrespectively of the walking direction. Even in absence of absolute heading information, angles between two body-attached inertial sensors can be estimated with an average accuracy of $<$2.56° at any point in time. This makes long-term biomechanical analysis possible in realistic outdoor settings.

References

[1] M. Iosa, P. Picerno, S. Paolucci, and G. Morone, "Wearable inertial sensors for human movement analysis," *Expert Rev. Med. Devices*, vol. 13, no. 7, pp. 641–659, Jul. 2016.

[2] J. F. Wagner, "About motion measurement in sports based on gyroscopes and accelerometers—An engineering point of view," *Gyroscopy Navigat.*, vol. 9, no. 1, pp. 1–18, 2018.

[3] P. Picerno, "25 years of lower limb joint kinematics by using inertial and magnetic sensors: A review of methodological approaches," *Gait Posture*, vol. 51, pp. 239–246, Jan. 2017.

[4] L. C. Benson, C. A. Clermont, E. Bošnjak, and R. Ferber, "The use of wearable devices for walking and running gait analysis outside of the lab: A systematic review," *Gait Posture*, vol. 63, pp. 124–138, Jun. 2018.

[5] M. Kok, J. D. Hol, and T. B. Schön, "Using inertial sensors for position and orientation estimation," *Found. Trends Signal Process.*, vol. 11, nos. 1–2, pp. 1–153, 2017.

[6] J. D. Hol, "Sensor fusion and calibration of inertial sensors, vision, ultra-wideband and GPS," Ph.D. dissertation, Dept. Elect. Eng. Autom. Control, Linköping Univ., Linköping, Sweden, 2011.

[7] J. Favre, B. M. Jolles, O. Siegrist, and K. Aminian, "Quaternion-based fusion of gyroscopes and accelerometers to improve 3D angle measurement," *Electron. Lett.*, vol. 42, no. 11, pp. 612–614, 2006.

[8] J. Cockcroft, J. H. Muller, and C. Scheffer, "A novel complimentary filter for tracking hip angles during cycling using wireless inertial sensors and dynamic acceleration estimation," *IEEE Sensors J.*, vol. 14, no. 8, pp. 2864–2871, Aug. 2014.

[9] W. H. K. de Vries, H. E. J. Veeger, C. T. M. Baten, and F. C. T. van der Helm, "Magnetic distortion in motion labs, implications for validating inertial magnetic sensors," *Gait Posture*, vol. 29, no. 4, pp. 535–541, Jun. 2009.

[10] G. Ligorio and A. Sabatini, "Dealing with magnetic disturbances in human motion capture: A survey of techniques," *Micromachines*, vol. 7, no. 3, p. 43, 2016.

[11] D. Roetenberg, H. J. Luinge, C. T. M. Baten, and P. H. Veltink, "Compensation of magnetic disturbances improves inertial and magnetic sensing of human body segment orientation," *IEEE Trans. Neural Syst. Rehabil. Eng.*, vol. 13, no. 3, pp. 395–405, Sep. 2005.

[12] H. Dejnabadi, B. M. Jolles, and K. Aminian, "A new approach to accurate measurement of uniaxial joint angles based on a combination of accelerometers and gyroscopes," *IEEE Trans. Biomed. Eng.*, vol. 52, no. 8, pp. 1478–1484, Aug. 2005.

[13] E. Dorschky, M. Nitschke, A.-K. Seifer, A. J. van den Bogert, and B. M. Eskofier, "Estimation of gait kinematics and kinetics from inertial sensor data using optimal control of musculoskeletal models," *J. Biomech.*, vol. 95, Oct. 2019, Art. no. 109278.

[14] D. Laidig, D. Lehmann, M.-A. Begin, and T. Seel, "Magnetometer-free realtime inertial motion tracking by exploitation of kinematic constraints in 2-DoF joints," in *Proc. 41st Annu. Int. Conf. IEEE Eng. Med. Biol. Soc. (EMBC)*, Jul. 2019, pp. 1233–1238.

[15] B. Fasel, J. Sporri, J. Chardonnens, J. Kroll, E. Müller, and K. Aminian, "Joint inertial sensor orientation drift reduction for highly dynamic movements," *IEEE J. Biomed. Health Informat.*, vol. 22, no. 1, pp. 77–86, Jan. 2018.

[16] J. K. Lee and T. H. Jeon, "IMU-based but magnetometer-free joint angle estimation of constrained links," in *Proc. IEEE SENSORS*, Oct. 2018, pp. 1–4.

[17] J. K. Lee, E. J. Park, and S. N. Robinovitch, "Estimation of attitude and external acceleration using inertial sensor measurement during various dynamic conditions," *IEEE Trans. Instrum. Meas.*, vol. 61, no. 8, pp. 2262–2273, Aug. 2012.

[18] D. Roetenberg *et al.*, "Joint angles and segment length estimation using inertial sensors," in *Proc. 3DMA-10 Meeting Tech. Group 3-D Anal. Hum. Movement ISB*, 2010, pp. 3–6.

[19] M. Kok, J. D. Hol, and T. B. Schön, "An optimization-based approach to human body motion capture using inertial sensors," *IFAC Proc. Volumes*, vol. 47, no. 3, pp. 79–85, 2014.

[20] J. Wendel and G. F. Trommer, "Tightly coupled GPS/INS integration for missile applications," *Aerosp. Sci. Technol.*, vol. 8, no. 7, pp. 627–634, Oct. 2004.

[21] S. Affatato, *Surgical Techniques in Total Knee Arthroplasty and Alternative Procedures*. Oxford, U.K.: Woodhead, 2015, ch. 2.

[22] J. Diebel, "Representing attitude: Euler angles, unit quaternions, and rotation vectors," Stanford Univ., Stanford, CA, USA, Tech. Rep. 2006, 2006.

[23] T. Seel, T. Schauer, and J. Raisch, "Joint axis and position estimation from inertial measurement data by exploiting kinematic constraints," in *Proc. IEEE Int. Conf. Control Appl.*, Oct. 2012, pp. 45–49.

[24] J. Nocedal and S. Wright, *Numerical Optimization* (Springer Series in Operations Research and Financial Engineering). New York, NY, USA: Springer, 2006.

[25] J. Clément, R. Dumas, N. Hagemeister, and J. A. de Guise, "Soft tissue artifact compensation in knee kinematics by multi-body optimization: Performance of subject-specific knee joint models," *J. Biomech.*, vol. 48, no. 14, pp. 3796–3802, Nov. 2015.

[26] E. S. Grood and W. J. Suntay, "A joint coordinate system for the clinical description of three-dimensional motions: Application to the knee," *J. Biomech. Eng.*, vol. 105, no. 2, pp. 136–144, May 1983.
[27] G. Wu *et al.*, "ISB recommendation on definitions of joint coordinate system of various joints for the reporting of human joint motion—Part I: Ankle, hip, and spine," *J. Biomech.*, vol. 35, no. 4, pp. 543–548, 2002.
[28] G. Wu and P. R. Cavanagh, "ISB recommendations for standardization in the reporting of kinematic data," *J. Biomech.*, vol. 28, no. 10, pp. 1257–1261, Oct. 1995.
[29] M. Norden, P. Müller, and T. Schauer, "Real-time joint axes estimation of the hip and knee joint during gait using inertial sensors," in *Proc. 5th Int. Workshop Sensor-Based Activity Recognit. Interact. (iWOAR)*, 2018, pp. 1–6.
[30] P. Muller, M.-A. Begin, T. Schauer, and T. Seel, "Alignment-free, self-calibrating elbow angles measurement using inertial sensors," *IEEE J. Biomed. Health Inform.*, vol. 21, no. 2, pp. 312–319, Mar. 2017.
[31] M. Kok *et al.*, "A scalable and distributed solution to the inertial motion capture problem," in *Proc. 19th Int. Conf. Inf. Fusion*, 2016, pp. 1348–1355.
[32] C. Forster, L. Carlone, F. Dellaert, and D. Scaramuzza, "On-manifold preintegration for real-time visual-inertial odometry," *IEEE Trans. Robot.*, vol. 33, no. 1, pp. 1–21, Feb. 2017.

Ive Weygers received the M.Sc. degree in engineering electronics-ICT from KU Leuven, Leuven, Belgium, in 2017. He is currently pursuing the Ph.D. degree with the Department of Movement and Rehabilitation Sciences, KU Leuven Campus Bruges. His Ph.D. thesis is on movement analysis with inertial sensors for assessment patients with musculoskeletal disorders in a hospital environment. His main supervisor is Prof. Dr. K. Claeys. He is currently with the Department of Movement and Rehabilitation Sciences, KU Leuven Campus Bruges under the supervisor of Prof. Dr. K. Claeys. His current research interest includes musculoskeletal disorders at the spine and the lower limb.

Manon Kok received the M.Sc. degrees in applied physics and in philosophy of science, technology and society, both from the University of Twente, Enschede, The Netherlands, in 2009 and 2007, respectively, and the Ph.D. degree in automatic control from Linköping University, Linköping, Sweden, in 2017.

From 2009 to 2011, she was a Research Engineer with Xsens Technologies. From 2017 to 2018, she was a Postdoctoral with the Computational and Biological Learning Laboratory, Machine Learning Group, University of Cambridge, Cambridge, U.K. She is currently an Assistant Professor with the Delft Center for Systems and Control, Delft University of Technology, The Netherlands. Her research interests include probabilistic inference for sensor fusion, signal processing, and machine learning.

Hans Hallez received the M.Sc. degree in computer science with the University of Ghent, Belgium, in 2003, and the Ph.D. degree in engineering with a specialty in biomedical engineering with the Medical Signal and Imaging (MEDISIP) Research Group, Faculty of Engineering, Ghent University in 2008.

He was a Postdoctoral Fellow with MEDISIP. He is currently an Assistant Professor with the KU Leuven Campus Bruges, Department of Computer Science. He is affiliated with the M-Group Research Group and with the DISTRINET Research Group. His research interests focuses on the development and design toward reliability and scalability of the signal/data processing (Machine Learning) in distributed sensor networks using embedded software engineering for healthcare and industrial applications. He is also interested in designing novel sensors and sensor methodologies for mechatronic systems in healthcare applications.

Henri De Vroey received the M.Sc. degree in physiotherapy and rehabilitation sciences from the KU Leuven, Belgium, in 2014.

After having worked for several years as a Clinical Practice Owner. He is currently pursuing the Ph.D. degree with the Department of Rehabilitation Sciences, KU Leuven Campus Bruges. His research interests and expertise lies within the field of functional recovery of patients who have orthopedic surgery to the lower extremity. More particularly, he is investigating the influence of implant design on the recovery of biomechanical function after knee arthroplasty surgery. He is also interested in full body motion analysis and the diagnostic capabilities it yields within the clinical practice setting.

Tommy Verbeerst received the M.Sc. degree in electrical engineering from KHBO, Ostend, Belgium, in 2008.

Since 2013, he has been working with KU Leuven and UC Vives. He is affiliated with the Department of Electrical Engineering (ESAT), KU Leuven Campus Bruges, Belgium. His current research interest includes the fields of engineering education, robotics, and machine-vision.

Mark Versteyhe received the M.Sc. degree in mechanical engineering and the Ph.D. degree in applied sciences, from KU Leuven in 1995 and 2000, respetively.

He has worked 16 years in industry in various functions linked to research and innovation. Since October 2016, he has been a Professor with KU Leuven's Faculty of Engineering Technology, Technology Campus Brugge, where he co-ordinates the research effort on connected mechatronics. His research focus lies in studying and applying the holistic paradigm of mechatronic system design. His special interest goes to "Dependability" which encompasses reliability-availability-robustness and security of a system and "Distributed Systems" which are treated as a complex ecosystem of machines and humans that are connected within the Industry 4.0 paradigm shift.

Kurt Claeys received the M.Sc. degree in musculoskeletal rehabilitation sciences and physiotherapy from the University of Ghent, Belgium, in 1993, and the Ph.D. degree in orthopedic manual therapist from the IRSK-WINGS institute Ieper, Belgium, in 2005, and the Ph.D. degree from KU Leuven, Belgium, in 2013.

He is currently a Professor and Chair of the Department Rehabilitation Sciences, KU Leuven Campus Bruges. Besides he is also works as a part-time in a private practice in Jabbeke, Belgium, as a specialized musculoskeletal physiotherapist. His research interest focuses on the biomechanical and clinical investigation of disturbed movement patterns in patients with musculoskeletal disorders at the spine and the lower limb. He is also interested in the development of movement analysis protocols for outside laboratory testing using wearable sensors.